EVALUATING SOIL-STRUCTURE INTERACTION EFFECTS USING DIMENSIONAL ANALYSIS

J. Zhang[1] and Y. Tang[2]

[1] *Assistant Professor, Dept. of Civil & Environmental Engineering, University of California, Los Angeles, USA*
[2] *Ph.D. Student, Dept. of Civil & Environmental Engineering, University of California, Los Angeles, USA*
Email: zhangj@ucla.edu, bytang@ucla.edu

ABSTRACT:

Soil-structure interaction can affect seismic responses of structures due to foundation flexibility and energy dissipation. The significance of these effects depends on the dynamic properties of foundation and structure as well as earthquake ground motions. This paper investigates the dynamic response of soil-foundation-structure interacting (SFSI) systems subjected to pulse-type near-fault ground motions. Through rigorous dimensional analysis, the normalized structural responses are represented in terms of dimensionless Π-products. This approach brings forward the self-similarity, an invariance with respect to scale or size, which decisively describes the interactive behavior of SFSI system. By allowing its foundation to translate and rotate, the normalized structural responses of a SFSI system are computed and compared with that of the fixed-base structure counterpart to evaluate the significance of soil-structure interaction. Extensive numerical simulations manifest the dimensionless parameters that dominate SSI effects and reveal the circumstances where SSI effects are of practical importance. For both linear and nonlinear structures with rocking foundation, the SSI effects are insignificant when the structure-to-pulse frequency ratio (Π_ω) is smaller than 1.5. They can amplify the structural response when Π_ω is higher than 1.5 and the structure-to-foundation stiffness ratio (Π_k) falls into certain range. SSI can result in significant large displacement demand on nonlinear structure. Furthermore, foundation rocking is able to enhance the SSI effects by shifting and enlarging the response amplification zone. The dimensional analysis offers a systematic way of evaluating SSI effects.

KEYWORDS: soil-structure interaction, near-fault ground motion, dimensional analysis

1. INTRODUCTION

The seismic response of a building or bridge can be significantly affected by the foundation and surrounding soil as well as the interaction between soil and structure. Soil-foundation-structure interaction effects, or so called soil-structure interaction (SSI) effects, have been observed and studied since 1930s. SSI has two aspects, kinematic interaction and inertial interaction. Kinematic interaction is characterized by modifying the free-field motion to be the base input motion. Inertial interaction is generally quantified by the period lengthening ratio and the foundation damping factor (Jennings and Bielak, 1973; Veletsos and Meek, 1974). This study will focus on the inertial SSI interaction, which is generally more important than kinematic interaction for structures with shallow foundation (Jennings and Bielak, 1973; Stewart et al., 1999a,b).

A large amount of research has been conducted to identify the factors that govern the inertial interaction effects, to determine the conditions under which the interaction effects are practically significant, and to develop simplified analytical procedures accounting for SSI effects. Jennings and Bielak (1973) found out that the interaction effects are influenced by the relative stiffness of the superstructure and its foundation, the structure height-to-foundation radius ratio, the fixed-base structural damping ratio as well as the structure-to-soil mass ratio. SSI occurs predominantly in the fundamental mode response of a structure and may be neglected for higher modes. They pointed out that whether SSI will amplify the structural response depends upon the modified natural frequency, the modified damping ratio, and the particular earthquake input. Veletsos and Meek (1974) identified the wave parameter, the height-to-radius ratio, and the ratio of exciting frequency to fixed-base fundamental frequency as the three most important parameters controlling inertial interaction phenomenon. They concluded that interaction is significant only for SFSI systems with a small wave parameter (< 20). Nevertheless, Veletsos and Meek (1974) did not define the circumstances where SSI will result in reduction or increase in structural response. Bielak (1975) revealed that amplified structural response may occur if SSI leads the system natural frequency approaching a prevailing ground motion frequency and neglecting interaction effects is not always conservative. Evaluating SSI effects through system identification analysis for 77 strong motion data sets at 57 building sites, Stewart et al. (1999a,b) identified the ratio of structure-to-soil stiffness, quantified by wave parameter, as the most critical one among all the important factors that influence the inertial interaction effects. They observed that inertial interaction effects are generally small for SFSI systems with a wave parameter bigger than 10. However, all the research work reviewed above has not defined clearly the circumstances where SSI effects are detrimental to structures. Neither has the dependency of SSI effects on the input ground motion been understood thoroughly. Therefore, more studies are needed to determine the conditions under which SSI will amplify or reduce the seismic responses of structures.

Among the large volume of earthquake records, typical near-fault ground motions are distinctive with the severe pulses in both velocity and displacement time histories (Bertero, 1976; Mavroeidis and Papageorgiou, 2003). Increasing database of near-fault ground motion records along with theoretical studies have confirmed and highlighted the presence of severe energetic pulses near the causative fault of an earthquake due to either rupture directivity or tectonic fling (Abrahamson, 2000). Alavi and Krawinkler (2004) demonstrated that structures with a period longer than the pulse motion period respond very differently from structures with a shorter period. Therefore, SSI effects might be important in estimating the seismic demands imposed by near-fault ground shaking since SSI tends to lengthen the fundamental natural period of a structural system.

In this paper, attempts are made to relate the SSI effects on structural responses directly to the mechanical properties of the SFSI system and the characteristic length scales of the ground motion through rigorous dimensional analysis. The influence of foundation rocking on the SFSI system is investigated. Furthermore, the conditions are recognized under which SSI effects can amplify the structural responses subjected to near-fault ground motions.

2. PULSE REPRESENTATION OF NEAR-FAULT GROUND MOTIONS

Near-fault ground motions may contain most of the seismic energy from the fault rupture arriving in a single coherent long-period pulse of motion. The pulse-type ground motions are particularly destructive to civil structures in a sense that they force the structures to dissipate the input energy with few large displacement excursions. Simple pulse models that capture the leading kinetic characteristics of near-fault ground motions were used widely for parametric studies of structures under earthquake (Alavi and Krawinkler, 2004; Makris and Black, 2004a,b; Kalkan and Kunnath, 2006; Mollaioli et al., 2006). The cycloidal pulses proposed by Makris and Chang (2000) are used in this study to resemble near-fault ground motions. These cycloidal pulses are physically realizable for their zero final velocity and finite acceleration.

A cycloidal pulse is fully defined with just two parameters, the acceleration amplitude, a_p, and period, T_p. As defined by Makris and Chang (2000), three distinct cycloidal pulse-type excitations are available, i.e. type-A, type-B and type-C_n pulses. Type-A pulse (one-sine acceleration pulse) results in a forward ground displacement that is not recovered at the end of earthquake. Type-A pulse is usually a result of fling step. Type-B pulse (one-cosine acceleration pulse) is characterized by a forward-back velocity time history and a fully recovered ground displacement at the end of earthquake. Type-C_n pulse exhibits n main cycles in its displacement history, where n could be equal to any integer. Figure 1 shows the cycloidal pulses that can be distinguished in real near-fault seismic motion records. Recent study by Mollaioli et al. (2006) showed that the cycloidal pulses are capable of representing the salient features of the structural response to near-fault ground motions within limitations. As far as displacement and input energy spectra are concerned, structural response to idealized pulses constitute a good approximation of those computed with recorded near-fault ground motions, for both the elastic and inelastic structures. Therefore, the pulse-type motions are used to evaluate the structural response of SFSI system in this paper.

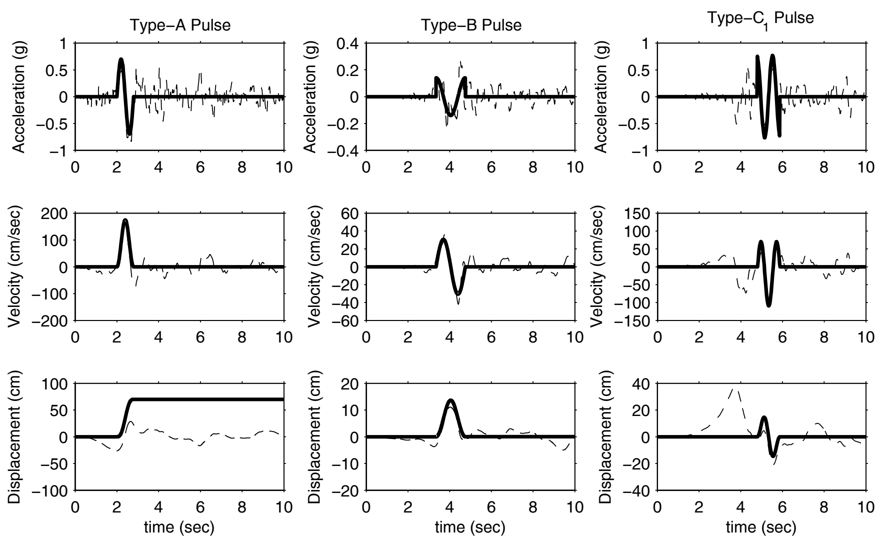

Figure 1 Near-fault ground motions (dashed lines) and their resemblance of pulse-type motions (solid lines). Left: Rinaldi (1994 Northridge); Center: Gilroy (1989 Loma Prieta); Right: New Hall (1994 Northridge)

3. DIMENSIONAL ANALYSIS OF STRUCTURE ON FLEXIBLE FOUNDATION SUBJECTED TO PULSE-TYPE EXCITATION

Previous studies (Jennings and Bielak 1973; Veletsos and Meek 1974) have also chosen dimensionless parameters to evaluate SSI effects based on physical observations and shown that the dimensionless formulation is able to offer insights into this complex problem. This study derives the dimensionless parameters through rigorous dimensional analysis and examines the significance of these parameters in terms of affecting the structural responses of SFSI systems.

3.1. Linear Structure on Flexible Foundation Subjected to Pulse-Type Ground Motion

A linear SFSI system can be simplified as a lumped 3DOF model as shown in Figure 2(a), where m_s, k_s, c_s, h_s denote the mass, stiffness, damping constants and height of the structure respectively, while m_f is the foundation mass. The three degrees of freedom are selected as the foundation displacement relative to the ground u_f, the foundation rocking angle θ, and the net structural displacement relative to ground u_s excluding rocking. For the translational DOF of foundation, k_f and c_f stand for the equivalent spring and dashpot values of soil-foundation respectively. k_θ and c_θ are respectively the equivalent spring and dashpot values of soil-foundation in the rotational DOF. The equations of motion of this lumped model subjected to ground motion, $\ddot{u}_g$, can be formulated as:

$$\begin{cases} m_s\left(\ddot{u}_s+h_s\ddot{\theta}\right)+c_s\left(\dot{u}_s-\dot{u}_f\right)+k_s\left(u_s-u_f\right)=-m_s\ddot{u}_g \\ m_f\ddot{u}_f-c_s\dot{u}_s+\left(c_s+c_f\right)\dot{u}_f-k_su_s+\left(k_s+k_f\right)u_f=-m_f\ddot{u}_g \\ m_sh_s\left(\ddot{u}_s+h_s\ddot{\theta}\right)+I_t\ddot{\theta}+c_\theta\dot{\theta}+k_\theta\theta=-m_sh_s\ddot{u}_g \end{cases} \tag{3.1}$$

where I_t denotes the sum of the mass moments of inertia of structure and foundation about their own centroidal axes.

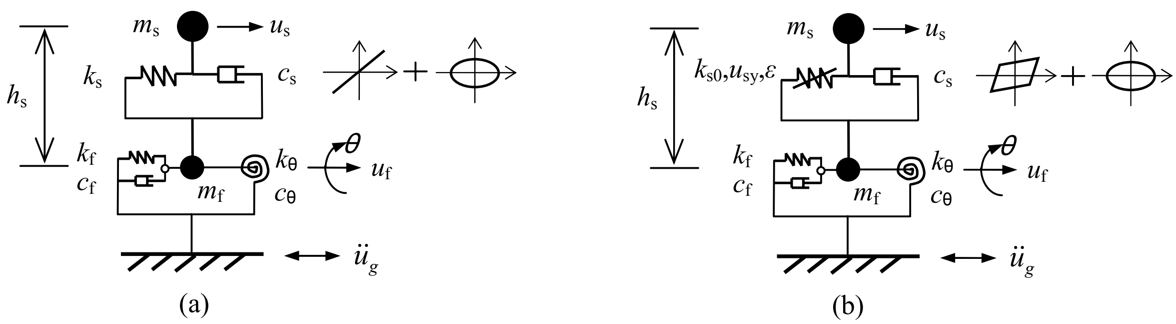

Figure 2 Lumped SFSI systems: (a) linear structure, (b) nonlinear structure

The structural response quantities of interest are the peak drift, $u_{drift}^{\max} = \max_t \left[|u_s(t) - u_f(t)| \right]$, which measures the structural deformation and the peak acceleration, $a_s^{\max} = \max_t \left[|\ddot{u}_s(t) + h_s \ddot{\theta}(t) + \ddot{u}_g(t)| \right]$, which is related to the maximum base shear force via $V_b^{\max} = m_s a_s^{\max}$. By dimensional analysis (Langhaar, 1951; Barenblatt, 1996; Tang and Zhang, 2008), the peak structural response to a pulse-type ground motion with acceleration amplitude a_p and circular frequency $\omega_p = 2\pi / T_p$ is formulated in the dimensionless form as:

$$\frac{u_{drift}^{\max}\omega_p^2}{a_p}, \frac{a_s^{\max}}{a_p} = \phi\left(\frac{\omega_s}{\omega_p}, \xi_s, \frac{m_f}{m_s}, \frac{k_f}{k_s}, \frac{c_f\omega_s}{k_f}, \frac{I_t}{m_s h_s^2}, \frac{k_\theta}{k_f h_s^2}, \frac{c_\theta \omega_s}{k_\theta} \right) \tag{3.2}$$

where $\omega_s = \sqrt{k_s / m_s}$ and $\xi_s = c_s / (2 m_s \omega_s)$ are respectively the natural circular frequency and damping ratio of the corresponding fixed-base structure. The characteristics of the acceleration pulse, a_p and ω_p, are selected as repeating variables in order to normalize the structural response to the length scale of the energy pulse in the ground motion, $L_e = a_p T_p^2 = 4\pi^2 a_p / \omega_p^2$ (Makris and Black, 2004a). Equation (3.2) indicates that the normalized maximum structural response ($\Pi_u \equiv u_{drift}^{\max}\omega_p^2 / a_p$ or $\Pi_a \equiv a_s^{\max} / a_p$) is a function of the normalized frequency ($\Pi_\omega \equiv \omega_s / \omega_p$), the fixed-base structural damping ratio ($\Pi_\xi \equiv \xi_s$), the foundation-to-structure mass ratio ($\Pi_m \equiv m_f / m_s$), the stiffness ratio ($\Pi_k \equiv k_f / k_s$), the normalized damping coefficient ($\Pi_c \equiv c_f \omega_s / k_f$), the normalized moment of inertia ($\Pi_I \equiv I_t / (m_s h_s^2)$), the normalized rocking-to-translation stiffness ratio ($\Pi_{k\theta} \equiv k_\theta / (k_f h_s^2)$), and the normalized dashpot ($\Pi_{c\theta} \equiv c_\theta \omega_s / k_\theta$) of foundation. The last three Π-terms (Π_I, $\Pi_{k\theta}$, and $\Pi_{c\theta}$) can be disregarded for cases with negligible foundation rocking, such as squat structures.

To investigate the SSI effects, it is necessary to express the fixed-base response of a structure also in a dimensionless form (Makris and Black, 2002a). The Π-terms that completely describe the fixed-base response of a linear structure are listed in Table 3.1 along with the Π-terms for flexible-base linear structures. The response ratios, $\Pi_{u,flex} / \Pi_{u,fixed}$ and $\Pi_{a,flex} / \Pi_{a,fixed}$, between the flexible-base structure and the fixed-base structure are reasonable measures of the SSI effects on structural response. A response ratio higher than the unity indicates that the SSI effects amplify the structural response while a response ratio below the unity indicates the reduced structural response due to SSI. SSI effects become insignificant when the response ratio is around one. It is observed that the response ratio $\Pi_{a,flex} / \Pi_{a,fixed}$ is approximately equal to $\Pi_{u,flex} / \Pi_{u,fixed}$ for ordinarily damped ($\xi_s \le 20\%$) linear SFSI systems since there exists $a_s^{\max} \approx \omega_s^2 u_{drift}^{\max}$ (Clough and Penzien, 1993).

Table 3.1 Dimensionless Π-terms of SFSI Systems

	Linear structure			Nonlinear structure		
	Fixed-base	*Flexible-base*	*Range*	*Fixed-base*	*Flexible-base*	*Range*
Π_u	$u_{drift}^{max}\omega_p^2/a_p$	$u_{drift}^{max}\omega_p^2/a_p$	N/A	$u_{drift}^{max}\omega_p^2/a_p$	$u_{drift}^{max}\omega_p^2/a_p$	N/A
Π_a	a_s^{max}/a_p	a_s^{max}/a_p	N/A	a_s^{max}/a_p	a_s^{max}/a_p	N/A
Π_ω	ω_s/ω_p	ω_s/ω_p	0.1 – 15	ω_{s0}/ω_p	ω_{s0}/ω_p	0.1 – 15
Π_ξ	ξ_s	ξ_s	0.02 – 0.1	ξ_s	ξ_s	0.02 – 0.1
Π_m	——	m_f/m_s	0.1 – 1	——	m_f/m_s	0.1 – 1
Π_k	——	k_f/k_s	0.1 – 1000	——	k_f/k_{s0}	0.1 – 1000
Π_c	——	$c_f\omega_s/k_f$	0.01 – 10	——	$c_f\omega_{s0}/k_f$	0.01 – 10
Π_I	——	$I_t/(m_s h_s^2)$	0.002 – 20	——	$I_t/(m_s h_s^2)$	0.002 – 20
$\Pi_{k\theta}$	——	$k_\theta/(k_f h_s^2)$	0.01 – 100	——	$k_\theta/(k_f h_s^2)$	0.01 – 100
$\Pi_{c\theta}$	——	$c_\theta\omega_s/k_\theta$	0.001 – 10	——	$c_\theta\omega_{s0}/k_\theta$	0.001 – 10
Π_{uy}	——	——	——	$u_{sy}\omega_p^2/a_p$	$u_{sy}\omega_p^2/a_p$	0.01 – 5
Π_ε	——	——	——	ε_s	ε_s	0.01 – 0.2

3.2. Nonlinear Structure on Flexible Foundation Subjected to Pulse-Type Ground Motion

Incorporating the bilinear hysteretic behavior of superstructure with Bouc-Wen model (Wen, 1976), a SFSI system can be modeled as a lumped 3DOF system as shown in Figure 2(b). Compared with the linear lumped model discussed in the preceding section, only the linear elastic structural spring is replaced by a Bouc-Wen bilinear spring characterized by the initial stiffness k_{s0}, the yield displacement u_{sy}, the ratio of post- to pre-yielding stiffness ε_s. Denoting u_s and u_f as the relative structural and foundation displacements to ground respectively, excluding the rigid body motion due to foundation rocking θ, the equations of motion of the nonlinear lumped 3DOF system can be written as:

$$\begin{cases} m_s\left(\ddot{u}_s + h_s\ddot{\theta}\right) + c_s\left(\dot{u}_s - \dot{u}_f\right) + \varepsilon_s k_{s0}\left(u_s - u_f\right) + (1-\varepsilon_s)k_{s0}u_{sy}z = -m_s\ddot{u}_g \\ m_f\ddot{u}_f - c_s\dot{u}_s + \left(c_s + c_f\right)\dot{u}_f - \varepsilon_s k_{s0}u_s - (1-\varepsilon_s)k_{s0}u_{sy}z + (\varepsilon_s k_{s0} + k_f)u_f = -m_f\ddot{u}_g \\ m_s h_s\left(\ddot{u}_s + h_s\ddot{\theta}\right) + I_t\ddot{\theta} + c_\theta\dot{\theta} + k_\theta\theta = -m_s h_s\ddot{u}_g \end{cases} \tag{3.3}$$

where z is a hysteretic variable governed by the ordinary differential equation shown below:

$$\dot{z} = [(\dot{u}_s - \dot{u}_f)/u_{sy}]\left\{1 - \left[0.5\cdot\text{sign}\left((\dot{u}_s - \dot{u}_f)z\right) + 0.5\right]\cdot|z|^{20}\right\} \tag{3.4}$$

Through rigorous dimensional analysis, it is revealed that the normalized structural response of the nonlinear lumped SFSI system, $\Pi_u = u_{drift}^{max}\omega_p^2/a_p$ or $\Pi_a = a_s^{max}/a_p$, is a function of ten dimensionless terms (also see in the sixth column of Table 3.1) as shown below:

$$\frac{u_{drift}^{max}\omega_p^2}{a_p}, \frac{a_s^{max}}{a_p} = \phi\left(\frac{\omega_{s0}}{\omega_p}, \xi_s, \frac{u_{sy}\omega_p^2}{a_p}, \varepsilon_s, \frac{m_f}{m_s}, \frac{k_f}{k_s}, \frac{c_f\omega_s}{k_f}, \frac{I_t}{m_s h_s^2}, \frac{k_\theta}{k_f h_s^2}, \frac{c_\theta\omega_s}{k_\theta}\right) \tag{3.5}$$

where $\omega_{s0} = \sqrt{k_{s0}/m_s}$ is the pre-yielding natural frequency of the fixed-base structure. The dimensionless terms that govern the normalized response of the corresponding fixed-base nonlinear structure is obtained through dimensional analysis and listed in the fifth column of Table 3.1. The ductility demand imposed on the nonlinear structure can be formulated as $\mu = u_{drift}^{\max}/u_{sy} = \Pi_u/\Pi_{uy}$. Similar to the linear structure, the response ratio between flexible-base response and fixed-base response of the nonlinear structure measures the SSI effects. It is worth noting that the response ratio of structural drift, $\Pi_{u,flex}/\Pi_{u,fixed}$, is equal to the response ratio of ductility demand, μ_{flex}/μ_{fixed}, provided that the normalized yield displacement, Π_{uy}, keeps the same. Unlike the linear SFSI system, the response ratio $\Pi_{a,flex}/\Pi_{a,fixed}$ is no longer close to $\Pi_{u,flex}/\Pi_{u,fixed}$ for nonlinear structure.

4. NUMERICAL RESULTS

In order to study the SFSI systems through numerical analysis, the range of interest for each independent Π-term needs to be determined first. Based on the 57 building sites studied by Stewart et al. (1999b) and the work done by Makris and Black (2000b), the ranges of the independent Π-terms are suggested in Table 3.1 for typical civil structures. In this study, the fixed-base structural damping ratio takes the constant 5%, i.e. Π_ξ=0.05 for both linear and nonlinear structures. A representative value of Π_m=0.25 is used since numerical results reveal that the SSI effects are insensitive to the foundation-to-structure mass ratio within the practical range.

Extensive numerical analyses are carried out to explore the SSI effects on the linear/nonlinear structural responses to pulse-type ground motions. Figure 3 plots the drift response ratio, $\Pi_{u,flex}/\Pi_{u,fixed}$, as a function of Π_ω, Π_k, and Π_c for both linear and nonlinear structures under type-B pulse excitation. The other dimensionless parameters used in this simulation are Π_{uy} = 0.05, Π_ε=0.05, Π_I=0.02, $\Pi_{k\theta}$=0.01, and $\Pi_{c\theta}$=0.001. The selection of the last three parameters allows the foundation to rock under earthquake motion, a common case for tall structures. The results show that SSI effects become negligible for Π_k>1000 as the response ratio approaching one while SSI effects tend to reduce the structural response when $\Pi_k\leq 1$. For linear structure, SSI may amplify the normalized drift in the neighborhood of $10\leq\Pi_k\leq 100$ when Π_ω>1 while the similar amplification occurs for nonlinear structure when Π_ω>3. This observation indicates that the structural yielding helps to reduce the effects of SSI when Π_ω<3 but can result in much larger displacement demand due to SSI effects when Π_ω>3. Similar trends associated with SSI effects are also identified in the acceleration response, except that the normalized drift usually increases to a larger degree than the normalized acceleration if there is amplification due to SSI. Furthermore, numerical results reveal that these trends are almost independent of the type of the input pulses. For nonlinear structures with large Π_{uy} (yield displacement) or Π_ε (post-yielding stiffness) the effects of SSI have similar trends observed for linear structure.

Foundation rocking is an important aspect of SSI, the significance of which is governed by the dimensionless terms Π_I, $\Pi_{k\theta}$, and $\Pi_{c\theta}$ in Table 3.1. By increasing any one of the three governing parameters, the foundation rocking will be constrained and the structural response will approach the situation without foundation rocking. Figure 4 compares the response ratios of normalized structural drifts of nonlinear structures with normalized foundation rotational spring of $\Pi_{k\theta}$=0.01 and $\Pi_{k\theta}$=100 under type-B pulse. For the latter, the rocking mode is constrained because of a very stiff rotational spring. As observed in Figure 4 by comparing these two cases, allowing foundation to rock can reduce the structural drift of the nonlinear structure when Π_ω<2. The structural drift of the flexible-base structure is typically lower than that of the fixed-base counterpart when $\Pi_k\leq 1$ indicating SSI is beneficial. However, this is not true if the foundation is not engaged in rocking motion since amplified responses due to SSI can be observed in the case of $\Pi_{k\theta}$=100. When the frequency ratio Π_ω>2, the foundation rocking results in shift of response amplification zone toward high stiffness ratio Π_k range and extension of amplification zone to the entire range of Π_c. The similar trend is also observed for linear structures (Tang and Zhang 2008).

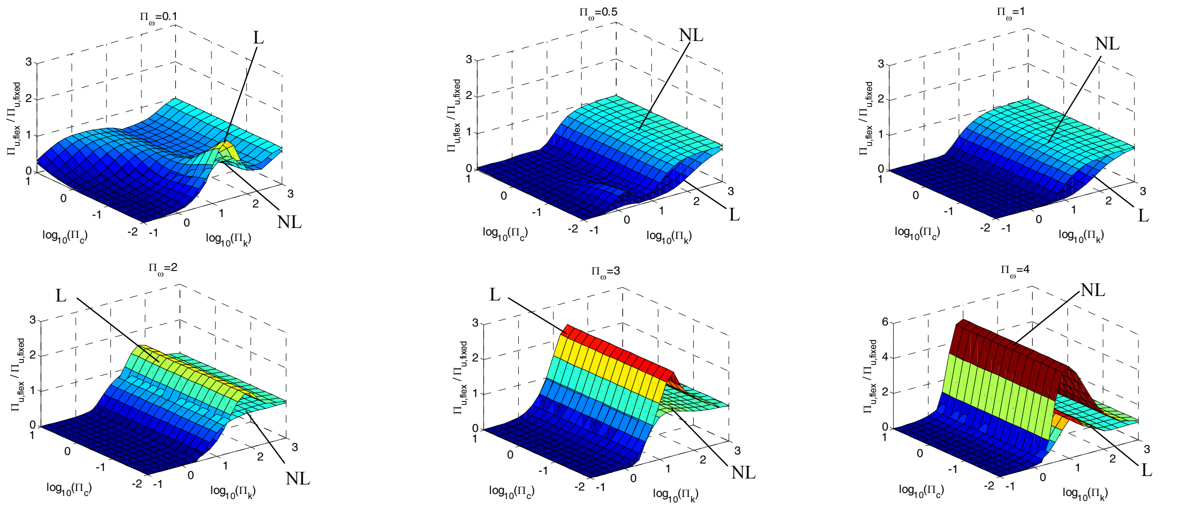

Figure 3 Response ratio of normalized structural drift between flexible- and fixed-base linear(L)/nonlinear(NL) lumped structures with Π_ξ =0.05, Π_{uy} = 0.05, Π_ε=0.05, Π_I=0.02, $\Pi_{k\theta}$=0.01, and $\Pi_{c\theta}$=0.001 for normalized frequency, Π_ω=0.1, 0.5, 1, 2, 3, and 4, under type-B pulse excitation

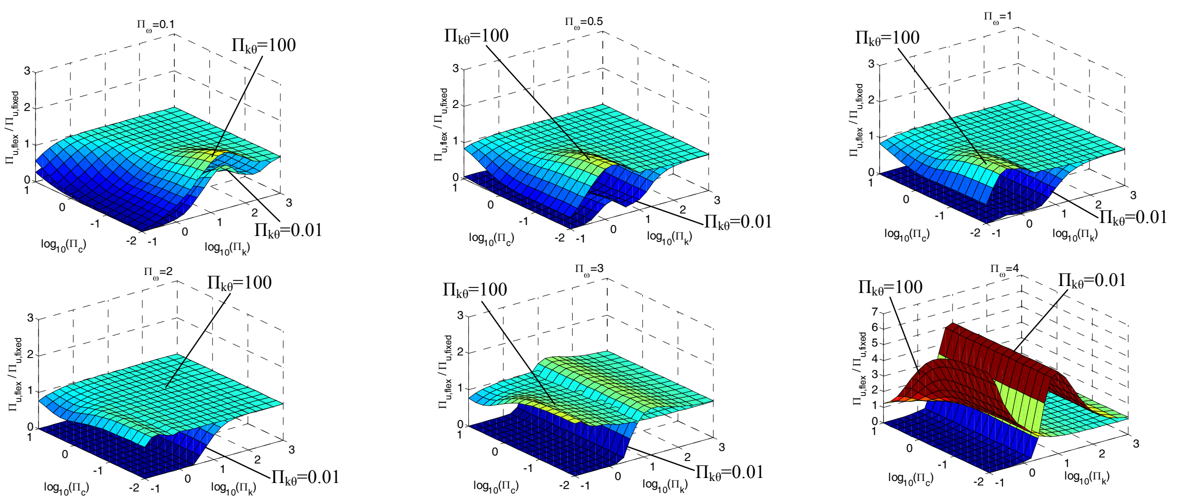

Figure 4 Response ratio of normalized structural drift between flexible- and fixed-base lumped nonlinear structures with Π_ξ =0.05, Π_{uy} = 0.05, Π_ε=0.05, Π_I=0.02, and $\Pi_{c\theta}$=0.001 for normalized frequency, Π_ω=0.1, 0.5, 1, 2, 3, and 4, under type-B pulse excitation: $\Pi_{k\theta}$=0.01 vs. 100

5. CONCLUSIONS

A new way is introduced in this paper to investigate the soil-structure interaction effects through rigorous dimensional analysis of the SFSI system combining the characteristics of the soil-foundation-structure system as well as the length scales of the input ground motion. Numerical simulations, interpreted in the framework of dimensional analysis, reveal that SSI effects highly depend on the pulse-to-structure frequency ratio, the foundation-to-structure stiffness ratio, the foundation rocking, and the development of nonlinearity in structure. The observations with the lumped SFSI models in this study can be applied to real structures provided that the seismic response of the structure is dominated by a certain vibration mode.

ACKNOWLEDGEMENT

Partial financial support for this study was provided by National Science Foundation under grant NEESR-SG: Seismic Behavior, Analysis and Design of Complex Wall Systems (Award #0421577).

REFERENCES

Abrahamson, N. (2000). Near-fault ground motions from the 1999 Chi-Chi earthquake. *Proceedings of U.S.-Japan Workshop on the Effects of Near-Field Earthquake Shaking*, San Francisco, California, 11–13.
Alavi, B., Krawinkler, H. (2004). Behavior of moment-resisting frame structures subjected to near-fault ground motions. *Earthquake Engineering and Structural Dynamics* **33:6**, 687–706.
Barenblatt, G.I. (1996). Scaling, Self-similarity, and Intermediate Asymptotics, Cambridge University Press, Cambridge, U.K.
Bertero, V.V. (1976). Establishment of design earthquakes—Evaluation of present methods. *Proceedings of International Symposium on Earthquake Structural Engineering*, St. Louis, Missouri, **Vol. 1**, 551–580.
Bielak, J. (1975). Dynamic behavior of structures with embedded foundations. *Earthquake Engineering and Structural Dynamics* **3:3**, 259–274.
Clough, R.W., Penzien, J. (1993). Dynamics of Structures, McGraw-Hill, New York, USA.
Jennings, P.C., Bielak, J. (1973). Dynamics of building-soil interaction. *Bulletin of the Seismological Society of America* **63:1**, 9–48.
Kalkan, E., Kunnath, S.K. (2006). Effects of fling step and forward directivity on seismic response of buildings. *Earthquake Spectra* **22:2**, 367–390.
Langhaar, H.L. (1951). Dimensional Analysis and Theory of Models, Wiley, New York, USA.
Makris, N., Chang, S. (2000). Effect of viscous, visco-plastic and friction damping on the response of seismic isolated structures. *Earthquake Engineering and Structural Dynamics* **29:1**, 85–107.
Makris, N., Black, C.J. (2004a). Dimensional analysis of rigid-plastic and elastoplastic structures under pulse-type excitations. *Journal of Engineering Mechanics* (ASCE) **130:9**, 1006–1018.
Makris, N., Black, C.J. (2004b). Dimensional analysis of bilinear oscillators under pulse-type excitations. *Journal of Engineering Mechanics* (ASCE) **130:9**, 1019–1031.
Mavroeidis, G.P., Papageorgiou, A.S. (2003). A mathematical representation of near-fault ground motions. *Bulletin of the Seismological Society of America* **93:3**, 1099–1131.
Mollaioli, F., Bruno, S., Decanini, L.D. and Panza, G.F. (2006). Characterization of the dynamic response of structures to damaging pulse-type near-fault motions. *Meccanica* **41:1**, 23–46.
Stewart, J.P., Fenves, G.L. and Seed, R.B. (1999a). Seismic soil-structure interaction in buildings. I: Analytical aspects. *Journal of Geotechnical and Geoenvironmental Engineering* (ASCE) **125:1**, 26–37.
Stewart, J.P., Seed, R.B. and Fenves, G.L. (1999b). Seismic soil-structure interaction in buildings. II: Empirical findings. *Journal of Geotechnical and Geoenvironmental Engineering* (ASCE) **125:1**, 38–48.
Tang, Y., Zhang, J. (2008). Inertial soil-structure interaction effects of structures on rocking foundations from dimensional analysis. *4th International Conference on Advances in Structural Engineering and Mechanics* (ASEM '08), Jeju, Korea.
Veletsos, A.S., Meek, J.W. (1974). Dynamic behaviour of building-foundation systems. *Earthquake Engineering and Structural Dynamics* **3:2**, 121–138.
Wen, Y.-K. (1976). Method for random vibration of hysteretic systems. *Journal of the Engineering Mechanics Division* (ASCE) **102:EM2**, 249–263.